AN INVESTIGATION OF THE BEHAVIOR OF THE SIMULTANEOUS THREE AXIS VIBRATION SYSTEM

G.K. Hobbs; Consultant

Robert Mercado; Santa Barbara Research Center

1. SUMMARY

Several high-rate production programs at Santa Barbara Research Center (SBRC) placed emphasis on finding economical and efficient screening systems. A quasi-random triaxial vibration system, including temperature cycling capability, was selected. Two Screening Systems, Inc., Multiaxial QRS-100s have been used at SBRC since June of 1980.

The systems have also been successfully used for locating defects. Some defects that have shown up during screening could not be found in the rework cycle under quiescent conditions nor could they be located using a single-axis vibration system in conjunction with thermal cycling.

To more thoroughly understand the behavior of the quasi-random multiaxis shaker, investigations of the motions in the time and frequency domains were undertaken, including the relationships between the three linear axes and between the three rotational axes. These investigations showed that the six axes of motion can be considered to be independent in terms of specimen response to the input motions.

2. THE SYSTEM INVESTIGATED

The QRS-100 is excited by pneumatically driven hammers which generate pulses. An ASD (or Fourier) analysis of these impacts shows a line spectrum with equally spaced lines. The fundamental frequency in the line spectra can be altered by changing the hammer velocity through varying the input air pressure. This is called smearing of the input. Each of the several (four are used as of this writing) hammers has a slightly different character and further smears the overall response of the QRS-100. The design of the structure between the hammers and the specimen to be screened further modifies the ASD as experienced by the specimen. The intervening structure is adjustable in several ways to allow variation in acceleration in the three axes and to control high-frequency rolloff. Substantial changes in the spectra can be attained by design changes in the structure between the hammers and the specimen.

Vibration is controlled by a microprocessor which controls the overall acceleration level. The air supply to the vibrators is modulated by a fast-acting digital flow valve which modulates the pressure in a quasi-random manner, resulting in spectral smearing of the input ASD. The overall grms input level is controlled using six multiplexed accelerometer feedback signals and maintaining an average as commanded by the program.

Temperature is controlled by an event programmer and a Research, Inc., temperature controller. The events programmer determines the rate of change of temperature, the temperature extremes and dwell times, and can also turn on the vibration controller and GN_2 purge (if desired) at specified times during the screen profile.

The mechanical shake table structure is mounted on air bags to allow motion of the entire system within the environmental chamber. The impacters are mounted to the outer ring on springs to provide adjustable high-frequency rolloff. The inner and outer rings are clamped together by an adjustable force elastomer interface to allow adjustment in distribution of energy between axes and also to

effect high-frequency rolloff. Finally, the tent-shaped fixture is bolted to the inner ring and there is a provision for mounting 12 specimens at a time. Figure 1 details a typical setup; further details of system configuration and performance are given [1, 2].

For the application at hand, the screen process was intended to expose part and workmanship defects. Note that there is no need to simulate actual field use conditions in a screen because once the flaws are removed under accelerated screening conditions, they will not fail under actual use conditions.

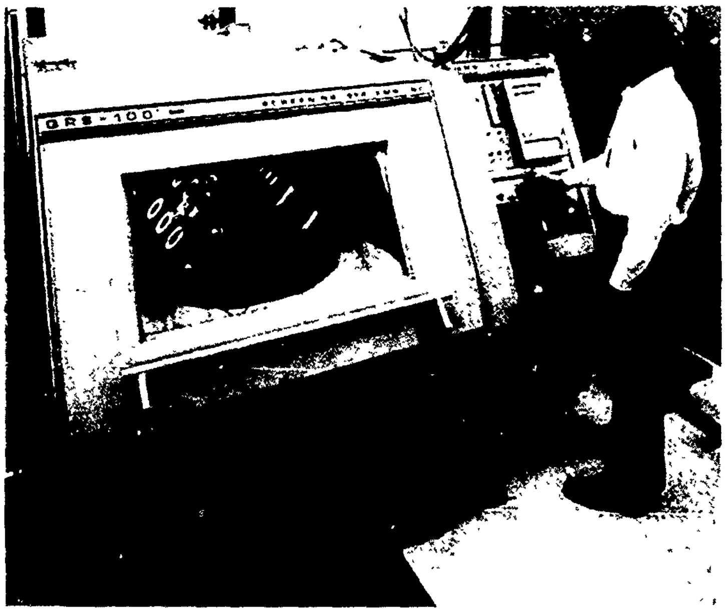

Figure 1. The QRS-100

3. EXPERIMENTS RUN, LINEAR MOTIONS

Reference 1 discussed screening results, fixture surveys, and the quasi-random response spectrum (QRRS). All of the results in Reference 1 were in terms of acceleration spectral density and were limited to linear motion only. Since knowledge of phase relationships between the axes was necessary to evaluate stresses due to multiaxial motion, including rotations, a more complete description of the motions was required.

The axes of motion are shown in Figure 2, which also shows the actuator arrangement. Note that the fixture is removed. Note also that the rear actuator is Screening Systems Model No. PV 1 5/8 - 1.6, whereas the other three are NAVCO MP 1-1 1/4.

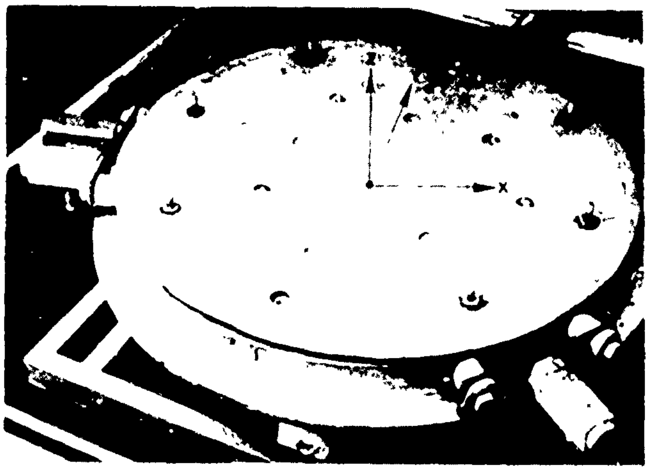

Figure 2. Axes and Actuator Arrangement

Each axis of motion of the QRS was examined to determine the statistical distribution of linear acceleration on the fixture. The probability and cumulative probability distributions were found to approximate the Gaussian distribution in both narrow- and broadband samples as previously reported [3].

For a sample of several locations on the fixture, auto- and cross-correlations were calculated. The autocorrelation functions implied a typical broadband random signal for all sample times and axes. The cross-correlations, however, were much more difficult to decipher as some samples appeared to be correlated and some did not. All showed evidence of the line spectra input from the actuators, and showed that the actuators had different repetition rates. The cross-correlation of different time samples taken at the same point always had varying character. Many cross-correlations were checked and none were the same, leading to the conclusion that the signals were nonstationary. These facts required the signals to be analyzed in the time domain.

In order to reduce the analysis problem as much as possible, only one actuator, the rear one in Figure 2, was utilized with the system run in the constant pressure (manual) mode. Only the motions of one location on the fixture were examined in detail and that was at one of the triaxial accelerometers used in the control system (Figure 3).

The signals from two accelerometers were fed into two charge amplifiers and tracking filters and were used to drive the vertical and horizontal axes of an oscilloscope. The bandpasses used in the investigations were 2 Hz, 10% of the center frequency, 100 Hz, and complete bandpass. Note that the two signals were not amplitude-controlled to be equal, so true Lissajous patterns were not formed. Since the only actuator used was mounted in the y direction, the y axis responses tended to exceed the x axis responses, which is not normally the case.

Figure 3. Control Accelerometer Arrangement

The tracking filters were first set to 2 Hz for a very close look at the behavior of the system. Note that the half-power bandwidth of a structure is generally much wider than this, so the specimen being screened responds to a much broader bandwidth (as discussed in [1]). For example, a structure with a natural frequency of 400 Hz, and with 4% of critical damping, has a half-power bandwidth of 32 Hz.

The actuator produces repeated impacts generating a line spectrum. The first line was at 68 Hz (for a given pressure) and the harmonics were found at exact integer multiples of 68 Hz. For the frequency range below 68 Hz and between the harmonics up to about 1000 Hz, there were essentially no signals when the analysis bandwidth was 2 Hz. At frequencies above 1000 Hz, system nonlinearities and slight changes in the actual repetition rate generated nearly continuous signals as the tracking filter was swept along. The ellipse drawn by the two

signals was found to be amplitude-modulated and to wobble at the lower frequencies (up to the fourth harmonic at 272 Hz). The amplitudes varied in time by factors of from 30% to 95%, and the angles of the principal axis varied about 5°. Above the fourth harmonic the ellipse was very unsteady and varied in amplitude and angle, with an ellipse principal axis varying 360°. (See Figures 4 and 5 for examples.)

Selection of a 10% bandwidth at center frequencies below the sixth harmonic (408 Hz) produced little change from the 2 Hz bandwidth, but above that frequency the difference was very great, as two or more lines of the spectra would pass through the filters. At these higher frequencies, the oscilloscope showed an elliptical outline with lines traced throughout the ellipse. The ellipse outline also changed with time to some extent. (See Figure 6.)

Examples of some of the phenomena are shown in Figures 4 through 9, all of which are annotated separately. Figure 4 illustrates a very narrow-band analysis at a harmonic of the repetition rate of the actuator, with the ellipse modulated and rotating; a double exposure of this type of figure is shown in Figure 5. Figures 6 and 7 illustrate the effect of a broader bandwidth than on Figure 4. Note that the gains used were always equal on the vertical and horizontal axes, but were changed as necessary to fill the frame. Figure 8 shows that using all four actuators rounds out the pattern. Figure 9 illustrates a bandwidth corresponding to 5% of critical damping.

The vector acceleration was studied mathematically in order to evaluate the probability distribution of the acceleration. A Monte Carlo model using three Gaussian distributions, each with 5.5 grms, was set up and run on an Apple II computer, and the resulting probability distribution is shown in Figure 10. Note that the distribution is similar to a lognormal distribution. The 1σ, 2σ, 3σ and 4σ points are shown on the figure. The "max acceleration" of 28.6g in the title block was used only for scaling the abscissa and was calculated as the 3σ

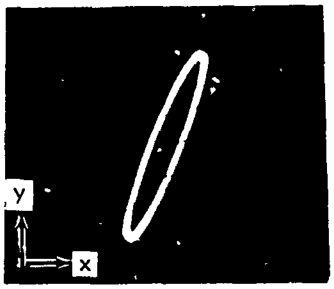

Figure 4. Experimental Results: Center Frequency, 409 Hz, Bandwidth 2 Hz, Modulated and Rotating, One Actuator

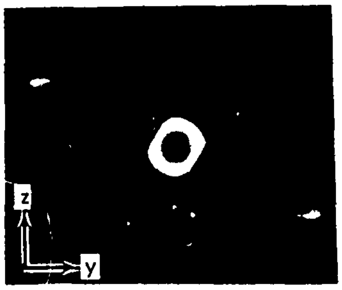

Figure 5. Experimental Results: Center Frequency, 346 Hz, Bandwidth 2 Hz, Four Actuators, Double Exposure

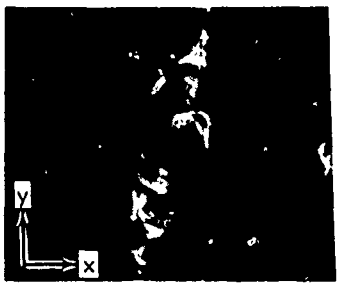

Figure 6. Experimental Results: Center Frequency, 409 Hz, Bandwidth 41 Hz, One Actuator

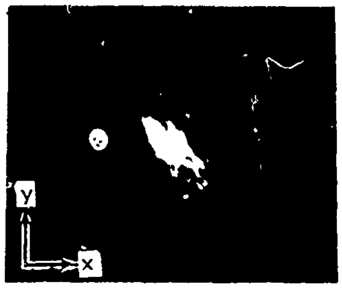

Figure 7. Experimental Results: Broadband, One Actuator

Figure 8. Experimental Results: Center Frequency, 433 Hz, Bandwidth 43 Hz, Four Actuators

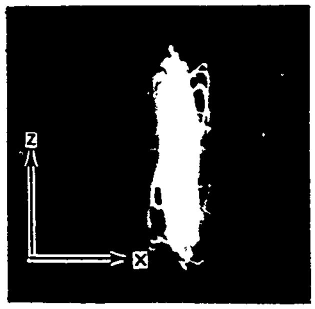

Figure 9. Experimental Results: Center Frequency, 433 Hz, Bandwidth 43 Hz, Four Actuators

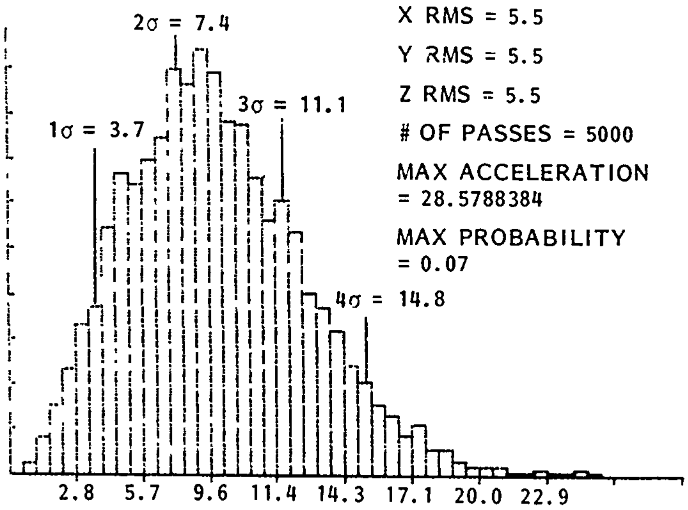

Figure 10. Vector Acceleration Probability Distribution

"vector" of the rms values for each axis as this was known to be an upper bound. Note that in 5000 samples the highest acceleration found was 25.7g.

The angular distribution of the acceleration vector was found to be uniform as the three distributions used had the same rms values. Other cases with non-equal rms values were run for completeness, but are not reported here.

4. CONCLUSION, LINEAR MOTIONS

Narrowband analysis of x and y, y and z, and x and z as pairs of signals shows that the signals are nonstationary and have no constant phase relationship even when only one actuator at a steady pressure is used. Analysis with a bandwidth of 10% of center frequency (about 5% of critical damping) with four actuators results in patterns where the vector acceleration occupies any part of an oblate spheroid in three space (recall that only one actuator in the y direction was used). This leads to the conclusion that the motions in the three axes are independent random variables. The dynamic response of a system exposed to the environment will accordingly be independently random in all three axes.

The oscilloscope patterns on a broadband basis show definitely preferred directions. However, any mode of a structure will respond principally to inputs within the half-power bandwidth of the mode and so broadband analysis is not really relevant for our purposes.

The vector acceleration was found to have an approximately lognormal distribution with the maximum value found in 5000 Monte Carlo trials being less than the 3σ "vector" sum of the rms values for each axis.

5. EXPERIMENTS RUN, ROTATIONAL MOTIONS

Preliminary studies had shown that substantial rotational accelerations existed. A more detailed study was undertaken in order to find the spatial and frequency relationships between the accelerations. The rotational accelerations were calculated from the linear accelerations as detailed in Figure 11.

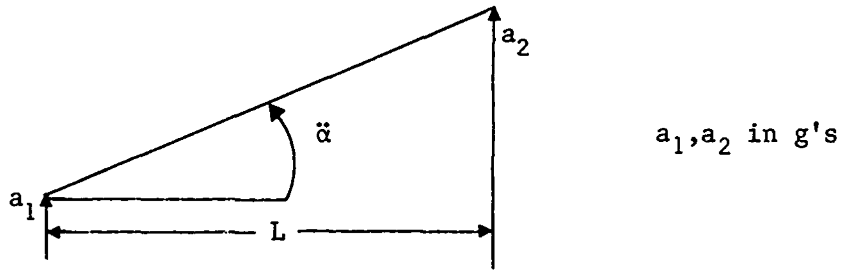

$$\ddot{\alpha} \text{ in rad/sec}^2 = \frac{(a_2 - a_1)}{L} \frac{g}{\text{in.}} \times \frac{386 \text{ in.}}{\text{sec}^2 g} = \frac{386(a_2 - a_1)}{L} \text{ rad/sec}^2 \quad (1)$$

when a is in g's and L is in inches

Figure 11. Rotational Acceleration Calculations

The angular acceleration spectral density (AASD) was calculated by spectral analysis of $\ddot{\alpha}$ rad/sec^2 and resulted in dimensional units of rad^2/sec^4-Hz. The dimension Hz results from division by the filter bandwidth. Two methods were used: digital real time analyzer (RTA), and narrowband analysis of each acceleration followed by summation (including phase angles) and then division by the filter bandwidth. Both techniques proved to be of value.

Prior to any data analysis all instrumentation was checked for proper level and phase relationships. All data was taken at the mounting interface of the unit being screened. All three rotational accelerations were stored on tape in raw linear acceleration form so that analysis in any form could be done later. All impacters were operational and both the constant pressure and automatic control modes were utilized.

When recording was complete, the next step was to make ASD plots using a real time analyzer and to make phase plots using a time series analyzer. Plots of ASD (linear) and phase angle between the two channels used for analysis were performed for many channels, two of which are shown in Figures 12 through 15. Note in Figures 12 and 13 that the ASD has a reasonably continuous distribution, in terms of the QRRS, considering that the analyzer utilized had a 13 Hz bandwidth. Note also that the two ASDs are somewhat different in terms of amplitude distribution. Similarly, each phase angle plot looked different except at a few frequencies as shown.

Further analysis of each acceleration was performed by use of a dual channel oscilloscope in two ways. A time domain photo of the filtered output from two in-line paired accelerometers 3.86 inches apart is shown in Figure 16. The center frequency is 735 Hz and the filter bandwidth is 15 Hz. Note that the phase angle between the signals is not constant.

Driving the oscilloscope with the filtered output on the vertical channels and with the sweep oscillator output on the horizontal channel resulted in Figure 17. The same type of pattern was evident at many other frequencies showing that the amplitude and phase angles were nonstationary.

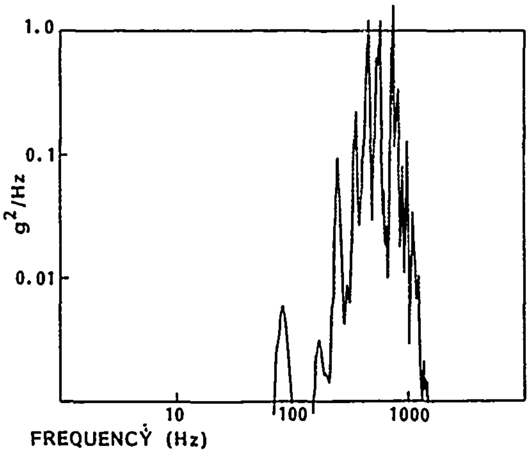

Figure 12. ASD Plot, Channel 2

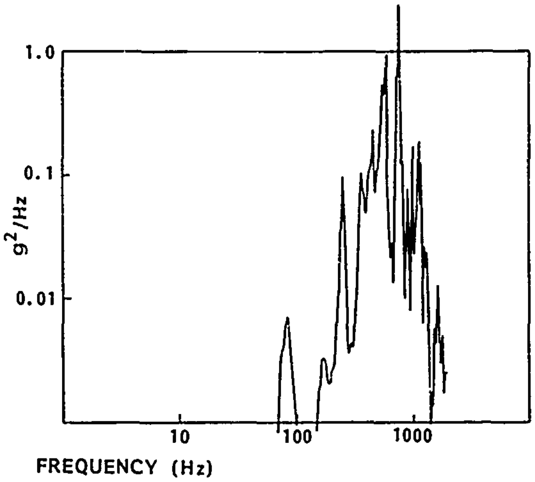

Figure 13. ASD Plot, Channel 4

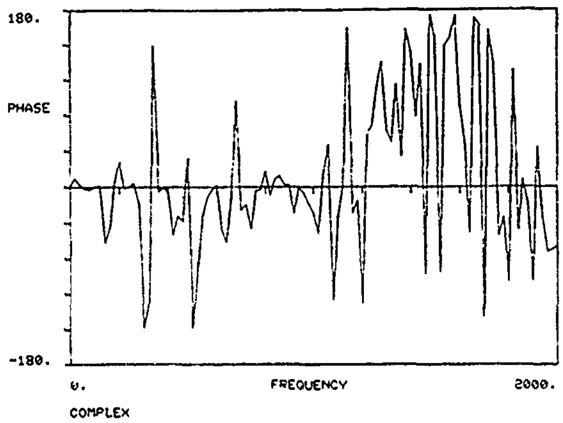

Figure 14. Phase Plot, Channels 2 and 4

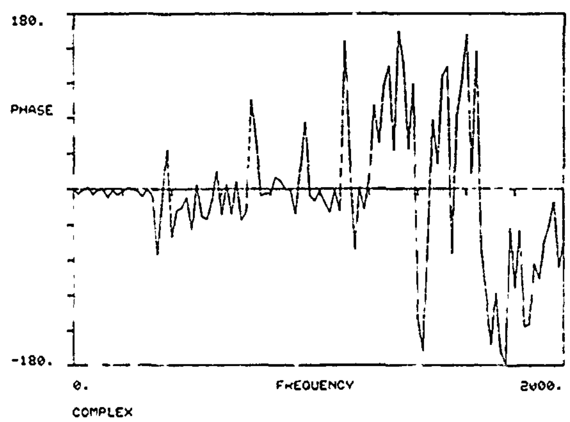

Figure 15. Phase Plot, Channels 2 and 4

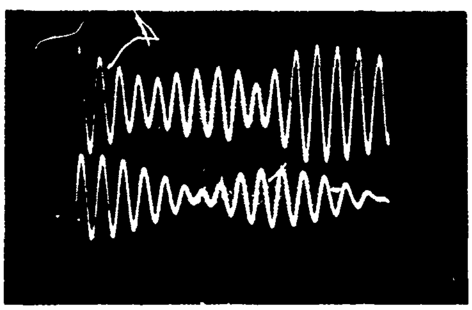

Figure 16. 735 Hz; 15 Hz Filter

Figure 17. 475 Hz; 15 Hz Filter

Another method of analysis was to set up the oscilloscope in the add mode (Figure 18) to obtain equation (1) (after inverting one signal from the tracking filter). Both narrowband signals could be observed on the oscilloscope and the resultant angular acceleration fed to the real time analyzer where the AASD can be observed and plotted if desired.

The AASD plot of the broadband output (i.e., without any filtering) is shown in Figure 19. The real time AASD was noted to vary by as much as 20 dB per second, again indicating nonstationary angular accelerations.

The final analysis of angular accelerations was done using the oscilloscope and driving the vertical and horizontal channels with two in-line accelerometers in order to see the relationships of linear and angular motion. A straight line

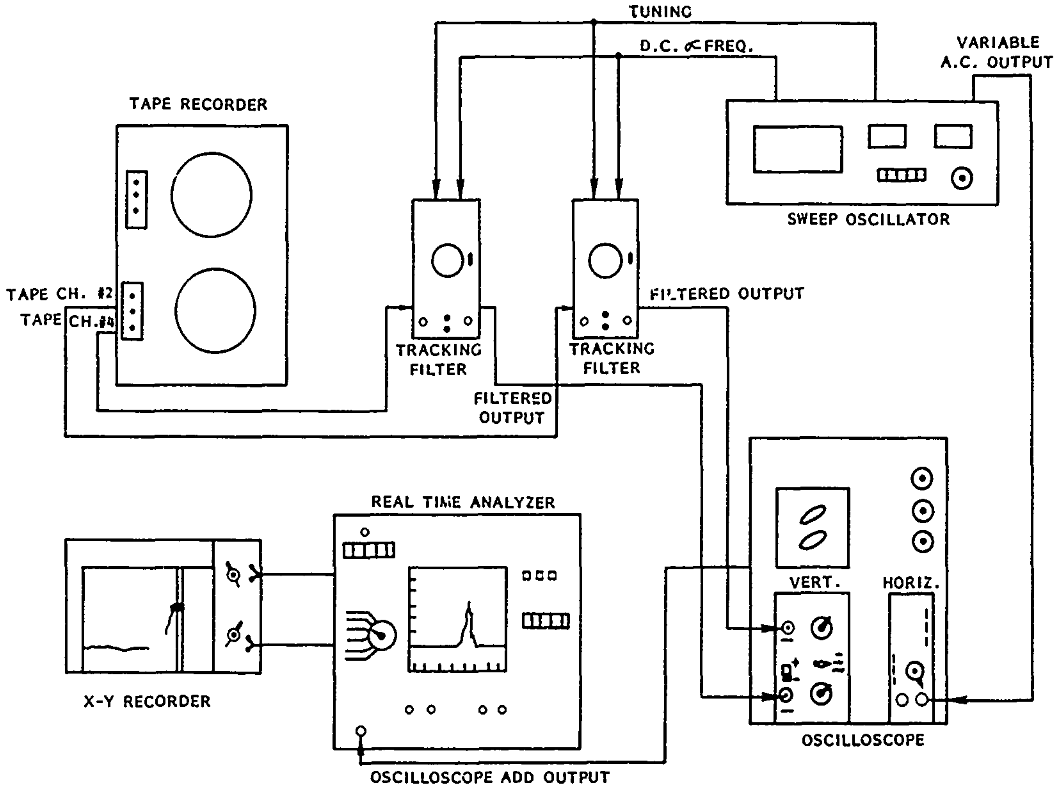

Figure 18. Add Mode Oscilloscope Setup (Rotational Analysis)

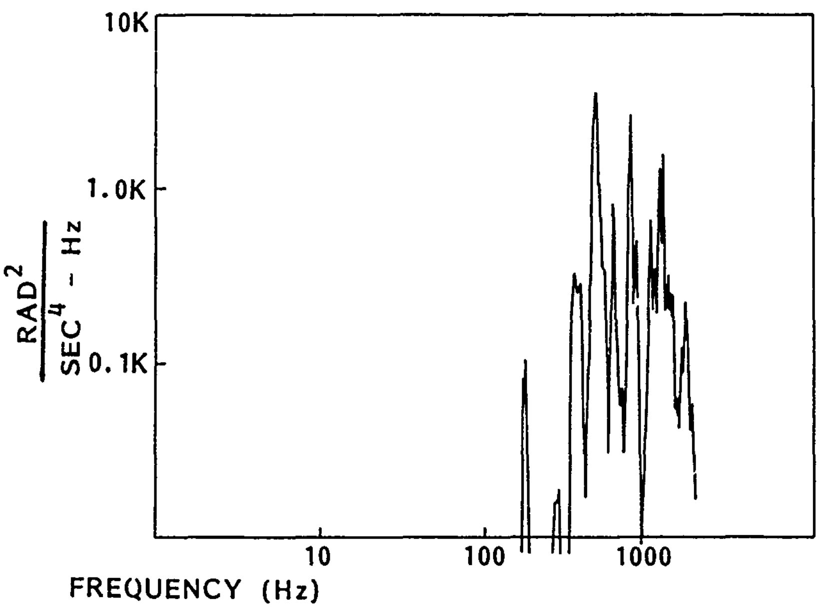

Figure 19. AASD Plot of Broadband Output

at 45° would indicate no rotation and purely in-phase motion. Other figures would indicate angular as well as linear motion. First, an electrodynamic shaker was analyzed with the accelerometers at the specimen mounting points and with a white noise input from 20 to 2000 Hz. The results are shown in Figures 20 through 22, which illustrate nearly perfect linear motion with very little rotation, which is supposed to be the case. A similar analysis was done on the QRS-100 run in the constant pressure mode and the results shown in Figures 23 through 25. The figures illustrate a large degree of out-of-phase motion at some times and in-phase at others, implying true six-degree of freedom motion.

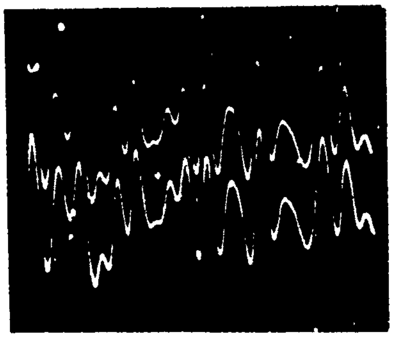

Figure 20. Two Broadband Waveforms on Electrodynamic Shaker

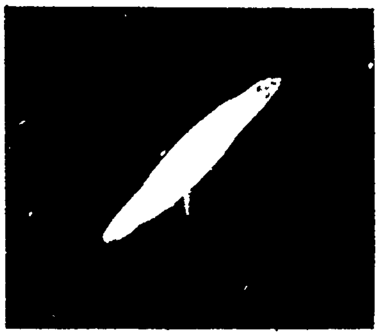

Figure 21. Narrowband (15 Hz) on Electrodynamic Shaker, Center Frequency 1000 Hz

Figure 22. 100 Hz Bandwidth on Electrodynamic Shaker, Center Frequency 1000 Hz

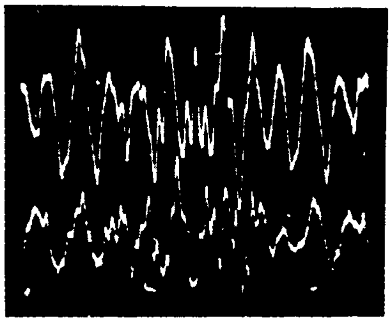

Figure 23. Two Broadband Waveforms on QRS-100 Systems

Figure 24. Narrowband (15 Hz) on QRS-100, Center Frequency 610 Hz

Figure 25. 100 Hz Bandwidth on QRS-100, Center Frequency 610 Hz

6. CONCLUSION, ANGULAR MOTION

The QRS-100 exhibits angular accelerations at nearly all frequencies when analyzed with a narrowband filter, and at all frequencies when analyzed with a filter corresponding to a typical structural half-power bandwidth.

7. SUMMARY AND AN EXAMPLE

The QRS-100 has accelerations in all six degrees of freedom as measured by a typical structural half-power bandwidth filter of 5% to 10% of the center frequency (2.5% to 5% critical damping). The motions are all nonstationary in time, have Gaussian distributions when measured independently, and are not correlated. The system therefore behaves as a six-axis shaker with all axes being independent.

This behavior explains the results of an investigation wherein a system which had failed screening on the QRS-100 with cracked solder joints would not exhibit anomalies when excited by a single-axis system. The specimen was excited in all principal axes on the single axis system at g levels from 1/2 grms to 15 grms at ambient, high and low temperatures, without intermittents being observed. Excitation by the QRS-100 at a 1 grms level at low temperature showed system intermittents about 92% of the time.

In this example, the six simultaneous axes of motion were just what was needed to cause the cracked solder joint to show an open condition. Many other examples of this type have occurred at SBRC. Further comparisons of single-axis shaker and QRS-100 shaker screening results are given in [1] and [2].

1. G.K. HOBBS, J.L. HOLMES, R. MERCADO 1982 SEECO 82, the Society of Environmental Engineers, London, England. Stress Screening Using Multiaxial Vibration.
2. G.K. HOBBS, R. MERCADO 1982 Reliability and Maintainability Symposium, Los Angeles, California. Quasi-Random Stress Screening Using the QRS-100.
3. A.J. CURTIS 1979 Hughes Aircraft Interdepartmental Correspondence. Analysis of Pneumatic Actuator (Baker Shaker) Vibration Signals.